Zonal slope prediction for open-loop adaptive optics

Chao Liu,[1,2,3] Lifa Hu,[1] Zhaoliang Cao,[1] Quanquan Mu,[1] and Li Xuan[1,*]

[1]*State Key Laboratory of Applied Optics, Changchun Institute of Optics, Fine Mechanics and Physics, Chinese Academy of Sciences, Changchun, Jilin 130033, China*

[2]*Graduate School of the Chinese Academy of Sciences, Beijing 100039, China*

[3]*e-mail: liuchao678@163.com*

**Corresponding author: xuanli@ciomp.ac.cn*

Received September 8, 2011; revised October 10, 2011; accepted October 10, 2011; posted October 14, 2011 (Doc. ID 154164); published November 15, 2011

We present what we believe to be the first results that obtained with the recursive least square zonal slope predictor working on an open-loop liquid-crystal adaptive optics system operating on astronomical implementation at visible and near infrared wavelength on a 1.23 m telescope. The system produces substantially better results than a direct open-loop correction based on previous measurement. A 27% relative gain in full-width at half-maximum and 30% relative gain in Strehl ratio are obtained. © 2011 Optical Society of America

OCIS codes: 010.1080, 230.3720, 010.1330.

The adaptive optics systems (AOS) have an inherent error source the time delay that results in the corrections always lagging behind the wavefront distortions. Fortunately, the deteriorative effect of time delay could be reduced by predictors. Indeed, atmospheric turbulence is predictable [1,2]. Predictors have already been studied in closed-loop AOS based on deformable mirrors (DM) [3–5]. In the open-loop regime, the artificial neural networks are used to predict turbulence wavefront slope [6,7]. However, they need hundreds of thousands of training data and are plagued by running into local minima in the training error surface [8]. Gibson, Barchers, and Rhoadarmer *et al.* [4,9,10] have shown the possibility to correct and predict the turbulent wavefront with the recursive least squares (RLS) algorithm [11]. In this Letter we describe a new spatiotemporal predictor that copes with the Shack–Hartmann wavefront sensor (SHWFS) slope values with the RLS algorithm and apply it to an open-loop AOS for astronomical implementation. Compared with the modal prediction method [12,13], it can take good advantage of the wind information. Therefore, it can acquire better predictive results.

The architecture of the zonal slope predictor is shown in Fig. 1. For each subaperture of the SHWFS, we use the slope values s_{ij} of itself and its neighbors (K subapertures for each frame of data) of the past M frames of data, each with a linear weight ω_{ij}, to predict the corresponding slope value s of the subaperture in the next N frame of data. It is

$$\hat{s} = \sum_{i=0}^{k-1}\sum_{j=0}^{m-1} \omega_{ij} s_{ij}. \tag{1}$$

The basic idea of deriving a good predictor is to obtain good series of these prediction coefficients which are obtained by minimizing the mean square prediction error. The prediction coefficients are updated for each recursive step and ultimately approach the most optimized prediction coefficients. The RLS zonal slope prediction procedure can be divided into two steps: the study step and the prediction step. In the study step, the prediction coefficients are updated. For the prediction of each subaperture, the import vector of the RLS predictor is

$$\underline{u}(n) = [s_{00} \cdots s_{0,M-1} s_{10} \cdots s_{K-1,M-1}]_n^T. \tag{2}$$

The import vector contains both the temporal and spatial information. T is the transpose of the vector and the underline indicates that it is a column vector in this Letter. The prediction coefficient vector that needs to be updated can be written as

$$\underline{\omega}(n-1) = [\omega_{00} \cdots \omega_{0,M-1} \omega_{10} \cdots \omega_{K-1,M-1}]_{n-1}^T. \tag{3}$$

Each element of the prediction coefficient vector represents the predictive contribution of the corresponding slope to the slope being predicted.

The prediction coefficient vector is updated through the recursive process: [11]

$$\begin{aligned}
\underline{k}(n) &= \frac{P(n-1)\underline{u}(n)}{\lambda + \underline{u}(n)^T P(n-1)\underline{u}(n)}, \\
P(n) &= \lambda^{-1}P(n-1) - \lambda^{-1}\underline{k}(n)\underline{u}(n)^T P(n-1), \\
\alpha(n) &= s(n+N) - \underline{u}(n)^T \underline{\omega}(n-1), \\
\underline{\omega}(n) &= \underline{\omega}(n-1) + \underline{k}(n)\alpha(n),
\end{aligned} \tag{4}$$

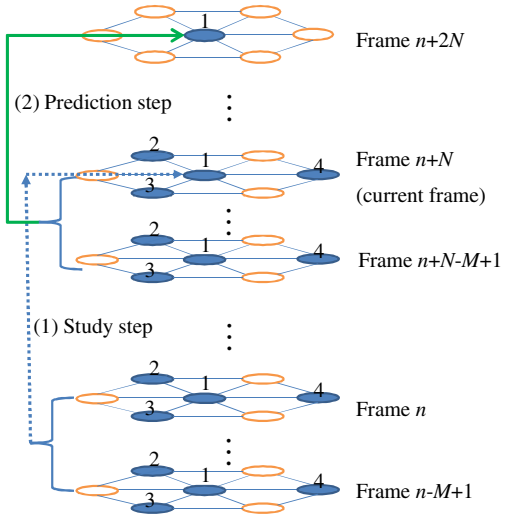

Fig. 1. (Color online) The two steps of the RLS prediction algorithm: the study step and the prediction step. The frame of subapertures showed here is only a fragment of that of the SHWFS frame.

where λ is the forgetting factor, $s(n+N)$ is the desired response. $s(n+N)$ is the actual newly measured slope value of the subaperture 1 of the current frame $n+N$ (see Fig. 1). In order to start the recursions, the initial values of $\underline{\omega}(0)$ and $P(0)$ have to be given. In the experiment, we take

$$\underline{\omega}(0) = 0, \qquad P(0) = \delta I, \tag{5}$$

where I is an identity matrix, δ is a large number that is bigger than $50/\sigma^2$, (σ^2 is the variance of import vector $\underline{u}$). After a recursion of Eq. (4) is finished, the prediction coefficient vector of a certain subaperture is updated.

In the prediction step, the newly updated prediction coefficient vector and the newly measured slope vector $\underline{u}(n+N)$ are used to predict the unknown slope values $s(n+2N)$ through

$$\widehat{s}(n+2N) = \underline{u}(n+N)^T \underline{\omega}(n). \tag{6}$$

This step is also illustrated in Fig. 1. The procedure including the study step and the prediction step continues until the prediction of all the effective slope values of a SHWFS frame is complete. Then, a frame of predicted slope values is achieved, which is expanded on the Zernike polynomials to drive the liquid crystal (LC) wavefront corrector [14]. Once a new frame of SHWFS measurement is acquired, the whole process mentioned above is repeated with n replaced by $n+1$.

The predictor was implemented on an open-loop LC adaptive optics system (OLAOS), which was mounted on the 1.23 m telescope of the CIOMP in Changchun, China. The performance of the predictor is compared with an ordinary controller that corrects directly based on SHWFS measurements, namely direct correction. The OLAOS is equipped with a two-axis tip-tilt mirror (TTM) with a diameter of 10 mm and a 256×256 pixels nematic pure-phase LC wavefront corrector (LWC). The central wavelength of the LWC is 785 nm. The light intensity with a waveband from 700 to 950 nm is propagated to the LWC to compensate the wavefront aberration and then to a science camera for imaging the observed star. The science camera is a DU897 EMCCD camera with 512×512 pixels. The other light intensity with a waveband from 400 to 700 nm is used to measure the turbulent phase with a 103-hexagonal-subaperture SHWFS. The SHWFS is equipped with a 64×64 pixel (2×2 binning) Andor DU860 EMCCD with a maximum EM gain of 1000. It has a sampling frequency of 910 Hz and an equivalent electronic noise level of one electron per pixel per frame. The global tilts, subtracted from the slope data measured by the SHWFS, are used to control the TTM by a proportional-integral (PI) controller working in closed-loop. The remaining slope data are applied to the predictor. Then, the predicted slope data are expanded on the Zernike polynomials to control the LWC in an open-loop manner. The calibration errors of the OLAOS are corrected. The registration error is very small and can be neglected. The main error of the OLAOS is the time delay error. The time delay is due to the exposure time of the SHWFS (1.1 ms), the SHWFS readout time (1.1 ms), calculating time (0.7 ms), transmission time (0.4 ms), and the LC response time (1.5 ms). The total delay time is 4.8 ms, which is nearly four sampling frames. Therefore, the prediction frame number N equals four in our experiments.

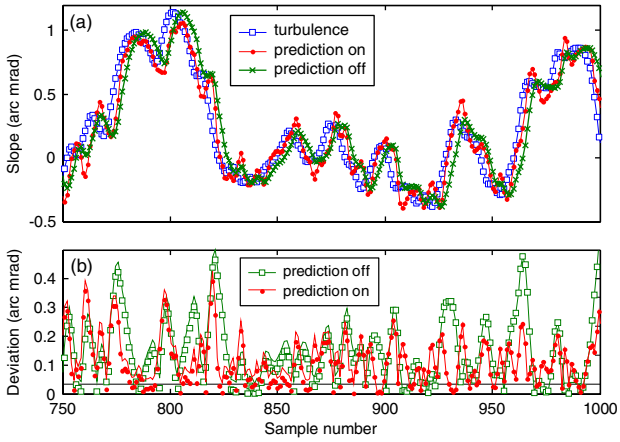

Fig. 2. (Color online) The sixty-eighth slope of turbulence, the corresponding direct corrections, predictions (a) and the deviations between the turbulence and the two corrections (b) are plotted as functions of the sample number.

The field experiment was carried out during the night of June 24, 2011. The star Polaris, with magnitude 1.96, was observed from 14h17 to 14h26 UT. The signal to noise ratio (SNR) of the SHWFS was about 60 and the estimated subaperture tip/tilt measurement error due to noise was about 0.03 arc mrad. In order to estimate the turbulence condition, three groups of turbulence data of the SHWFS measurements were recorded to estimate the Fried parameter r_0 and Greenwood frequency f_g. The average r_0 at 0.55 μm was 5 cm and the mean f_g was 60 Hz.

Thereafter, the correction experiments without and with prediction were carried out. The forgetting factor λ was 0.999. Because of the calculation complexity, only eight subapertures (four in each frame, $K = 4$) of the last two frames ($M = 2$) were used to predict. Figure 2(a) shows the turbulence, the direct corrections and the predictions of a random selected slope (the sixty-eighth slope) of the SHWFS varying with the sampling number. The correlation coefficients between the turbulence and direct corrections or predictions illustrated in Fig. 2(a)

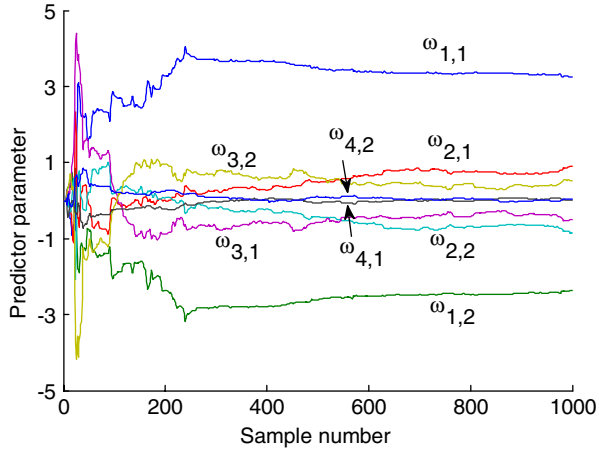

Fig. 3. (Color online) Convergence of the predictor parameters for the sixty-eighth slope.

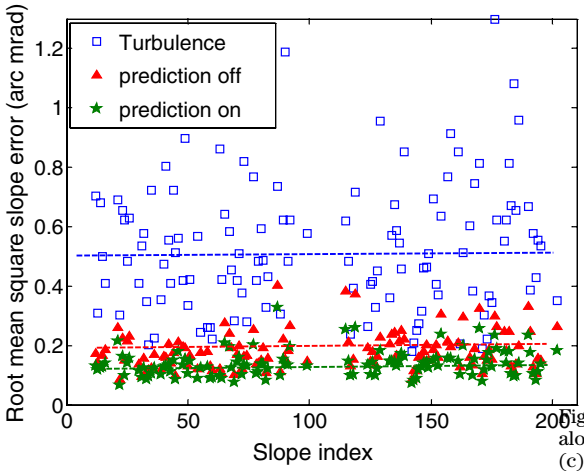

Fig. 4. (Color online) The root-mean-square slope error versus the WFS slope index (the first half slopes are x slopes and the last half slopes are y slopes).

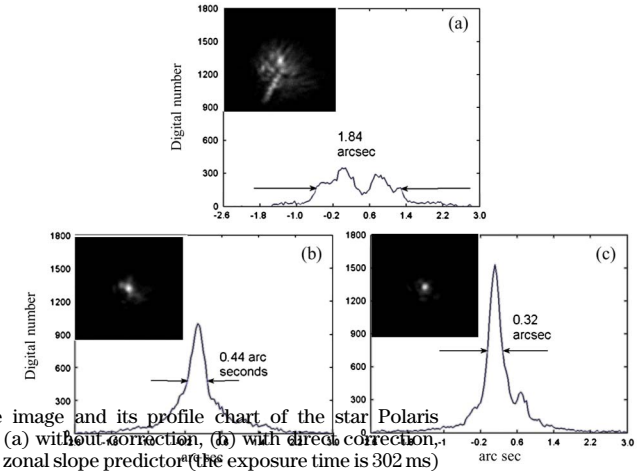

Fig. 5. The image and its profile chart of the star Polaris along y axis (a) without correction, (b) with direct correction, (c) with RLS zonal slope predictor (the exposure time is 302 ms) (Media 1).

are 0.89 and 0.95, respectively. The deviations of the predictions from turbulence were much smaller than that of the direct corrections from turbulence [see Fig. 2(b)]. Therefore, the direct corrections were always lagging behind the turbulent distortions while the predictions were much closer to the turbulent distortions. The convergence of the corresponding prediction coefficients is shown in Fig. 3. After about 700 recursions, all the prediction coefficients became steady. We also have confirmed that the prediction coefficients of the other slopes were all convergent after 700 recursions. The prediction results of each slope of the SHWFS are shown in Fig. 4. The mean slope value was about 0.5 arc mrad before correction. After direct correction, the residual mean slope value decreased to 0.19 arc mrad. Furthermore, the residual slope error decreased to 0.14 arc mrad after applying the prediction. A relative gain of about 26% in reducing residual slope value caused by time delay is achieved.

Before correction, the full-width at half-maximum (FWHM) of the star image of Polaris was 1.84″ and the Strehl ratio (SR) (550 nm) was 0.02 [See Fig. 5(a)]. After direct correction, the FWHM of the star image improved to 0.44″ and the SR increased to 0.12 [See Fig. 5(b)]. After appling the prediction technique, the FWHM of the image improved further to 0.32″ and the SR increased to 0.16 [See Fig. 5(c)]. Therefore, compared to direct correction, 27% relative gain in FWHM and 30% relative gain in SR have been achieved with the zonal slope prediction technique. A video about the Polaris image is also provided (first $1^{st} \sim 2^{nd}$ second: without correction; $3^{rd} \sim 5^{th}$ second: direct correction; $6^{th} \sim 8^{th}$ second: with prediction).

In conclusion, we have shown the feasibility of the zonal slope predictor used in an OLAOS. A 30% relative gain in SR has been achieved. It needs to be pointed out that the predictor is still in a low prediction regime. First, it is due to the long time delay of the OLAOS. If the time delay could be decreased, the prediction results would be improved. Second, due to the calculation complexity, only two SHWFS frames were used. In fact, using more frames and more subapertures in each frame would result in a more accurate predictor. The graphic processing unit that has powerful parallel calculation ability is currently under our consideration. In this case, more slope values could be used to improve the prediction results.

This work is supported by the National Natural Science Foundation of China (NSFC) (No. 60 736 042, No. 60 578 035 and No. 11 174 279).

References

1. C. Schwartz, G. Baum, and E. N. Ribak, J. Opt. Soc. Am. A **11**, 444 (1994).
2. G. J. Aitken and D. McGaughey, in *Proceedings of Topical Meeting on Adaptive Optics* (1995), Vol. 54, p. 89.
3. W. Wild, Opt. Lett. **21**, 1433 (1996).
4. B. L. Ellerbroek and T. A. Rhoadarmer, Math. Comput. Modell. **33**, 145 (2001).
5. L. Poyneer and J. Véran, J. Opt. Soc. Am. A **25**, 1486 (2008).
6. M. Jorgenson and G. Aitken, Opt. Lett. **17**, 466 (1992).
7. D. Montera, B. Welsh, M. Roggemann, and D. Ruck, Appl. Opt. **36**, 675 (1997).
8. P. McGuire, T. Rhoadarmer, H. Coy, J. Angel, and M. Lloyd-Hart, Proc. SPIE **4007**, 682 (2000).
9. J. S. Gibson, C.-C. Chang, and B. L. Ellerbroek, Appl. Opt. **39**, 2525 (2000).
10. J. D. Barchers, Appl. Opt. **43**, 3708 (2004).
11. S. Haykin, ed., *Adaptive Filtering Theory* (Prentice Hall, 2002).
12. C. Dessenne, P. Y. Madec, and G. Rousset, Opt. Lett. **22**, 1535 (1997).
13. C. Dessenne, P. Y. Madec, and G. Rousset, Opt. Lett. **24**, 339 (1999).
14. C. Liu, L. Hu, Q. Mu, Z. Cao, and L. Xuan, Appl. Opt. **50**, 82 (2011).